

# Multiple transitions in poly(allylbenzene): 2. Dielectric relaxations: relationship between structure and properties

Gisele Boiteux-Steffan, Gerard Seytre and Georges Vallet

Laboratoire d'Etudes des Matériaux Plastiques et des Biomatériaux 1-UA CNRS 507,  
Université 'Claude Bernard' Lyon 1, 43 Boulevard du 11 Novembre 1918, 69622  
Villeurbanne Cedex, France

and Daniel Chatain and Colette Lacabanne

Laboratoire de Physique des solides associé au CNRS, Université Paul Sabatier, 118  
Route de Narbonne, 31062 Toulouse Cedex, France  
(Received 5 June 1985; revised 25 February 1985)

The relaxations associated with the phase transitions observed in poly(allylbenzene) have been investigated by dielectric spectroscopy. A morphological model is proposed to describe the fine structure of glass and liquid-liquid transitions and a correlation is established between the polymer structure and several of its properties.

(Keywords: poly( $\alpha$ -olefin); poly(allylbenzene); thermally stimulated depolarization; relaxation spectrum; transition physico-chemical changes; morphological model)

## INTRODUCTION

Poly(allylbenzene) is a new dielectric material<sup>1</sup> which exhibits at  $T = 20^\circ\text{C}$  and  $N = 1$  kHz a good dielectrical constant ( $\epsilon' = 3$ ) and low dielectrical losses ( $\text{tg } \delta = 5 \times 10^{-4}$ ). The molecular structure of this polymer and its thermophysical properties were described in previous papers<sup>2,3</sup>.

Differential thermal analysis (d.t.a.) and differential scanning calorimetry (d.s.c.) have been used to show two unidentified transitions between  $120^\circ\text{C}$ – $150^\circ\text{C}$  ( $T_g = 59^\circ\text{C}$  and  $T_m = 204^\circ\text{C}$ ). Dilatometric measurements and thermal mechanical analysis have confirmed the existence of the  $T_g$  and the transitions around  $T = 120^\circ\text{C}$  and  $150^\circ\text{C}$ . Inverse gas chromatography clearly indicates two glass transitions around  $T = 51^\circ\text{C}$  and  $T = 70.5^\circ\text{C}$ . Shrinkage of the volume  $V_g$  occurs up to  $130^\circ\text{C}$  and is related to a modification of solvent accessibility towards sorption sites.

These transitions should be detectable by dielectric spectroscopy: d.c. and a.c. measurements as well as by thermally stimulated depolarization techniques.

In the paper presented here, we will analyse the results of these measurements and propose a morphological model which explains the observed behaviour of poly(allylbenzene).

## EXPERIMENTAL

### Samples

The poly(allylbenzene) films  $A_f$  were obtained by moulding in vacuum at temperature  $T = 204^\circ\text{C}$  at a pressure  $P = 590 \times 10^4 \text{ N m}^{-2}$ .

For a.c. and d.c. measurements sandwich-type samples were prepared by vacuum evaporation of aluminium electrodes. For thermally stimulated depolarization (t.s.d.) experiments, poly(allylbenzene) was studied on 10 mm square film or 12 mm diameter pressed pellets  $A_p$ .

These samples were not metallized, to avoid space carrier effects during the measurements.

### D.c. experiments

The sample was polarized in a thermoregulated cell<sup>4</sup> at  $150^\circ\text{C}$  in a field of  $4.7 \times 10^6 \text{ V m}^{-1}$ . The decay current was measured with a Keithley 642 Electrometer and registered until steady-state current was achieved. Then the temperature was lowered gradually to room temperature by  $10^\circ\text{C}$  steps, with an electric field applied constantly to the sample.

### A.c. experiments

The measurements were carried out in the thermoregulated cell previously described<sup>1</sup>, in vacuum of  $10^{-5}$  mm Hg, with a General Radio 1621 bridge in the low frequency range of  $10$ – $10^5$  Hz.

### Thermally stimulated currents

The samples were polarized under a blocking contact<sup>5</sup> with the field  $= 2 \times 10^6 \text{ V m}^{-1}$  for two minutes at various temperatures  $T_p$ , in a dried nitrogen atmosphere at a pressure of 200 torr in the measurement cell described before<sup>5</sup>. The temperature was then lowered to  $T_0 \ll T_p$  at which any molecular motion is frozen. At  $T_0$ , the electric field was removed and the thermocurrent  $J$  and the temperature  $T$  were recorded against time  $t$  while the sample was heated at a constant rate  $0.7^\circ\text{C min}^{-1}$ , so that the experiments are equivalent to a dynamic study carried out at  $10^{-3}$  Hz. The current was measured with a Cary 401 electrometer. We have verified the ohmic behaviour of the sample keeping in mind the problem of space carrier effects.

Thermal sampling technique was used for analysis complex t.s.c. spectra. The polarization field was applied for 2 min at the temperature  $T_p$  ( $-10^\circ\text{C} < T_p < 140^\circ\text{C}$ ) and then removed at ( $T_p - 10^\circ\text{C}$ ) which was kept constant for

another 2 min. Afterwards the t.s.c. experiments were carried out as usual.

## RESULTS

### D.c. study

A resistivity  $\rho$  versus  $1/T$  plot is shown in Figure 1. One can distinguish two temperature ranges with different activation energy of conductivity. Below  $T = 100^\circ\text{C}$ , activation energy can be estimated at  $\sim 3.6$  eV, while above  $100^\circ\text{C}$  activation energy decreases to 1.0 eV. This indicates an increase in the mobility of the charge carriers due to a drop in the potential barriers when passing over the glass transition of the material as the medium becomes less viscous.

### Dielectric measurements

The results are presented as plots of isochronous  $\text{tg } \delta$  versus temperature (Figure 2). Between  $-130^\circ\text{C}$  and  $160^\circ\text{C}$ , one can observe a  $\gamma$  relaxation around  $T = -110^\circ\text{C}$ . This is probably due to the movement of the phenyl groups. Such a  $\gamma$  relaxation was also observed for polystyrene around  $T = -100^\circ\text{C}$  in dynamic mechanical and dielectrical experiments<sup>6,7</sup>.

The  $\beta$  relaxation associated with the glass transition of the material is observed in the temperature range 55 to  $180^\circ\text{C}$ . The activation energy, as determined from the plot of log frequency maximum versus inverse temperature is 3.6 eV.

When compared with polystyrene, the  $\gamma$  and  $\beta$  relaxations of poly(allylbenzene) occur at lower temperatures. This can be attributed to the higher mobility of the

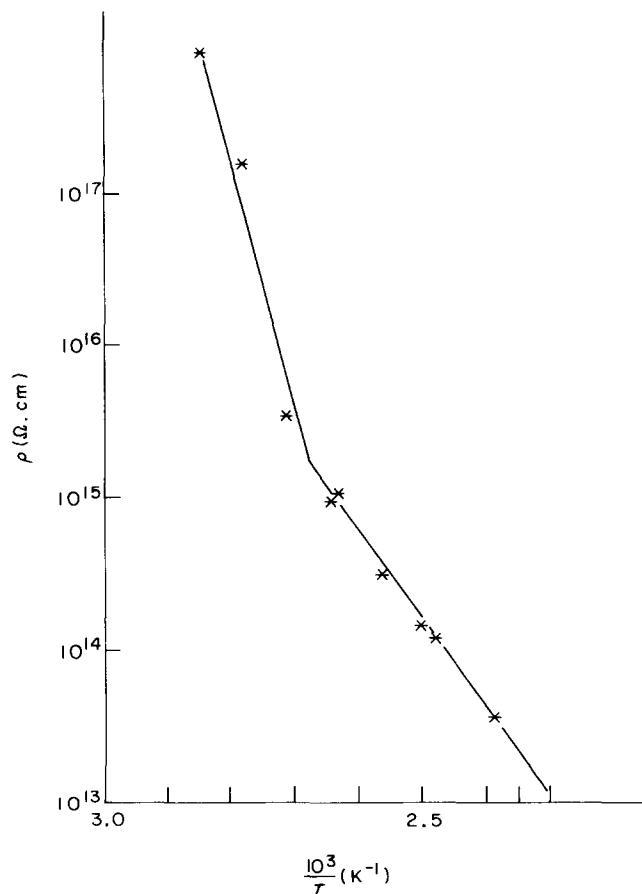


Figure 1 Variation of resistivity versus  $10^3/T$  in poly(allylbenzene)

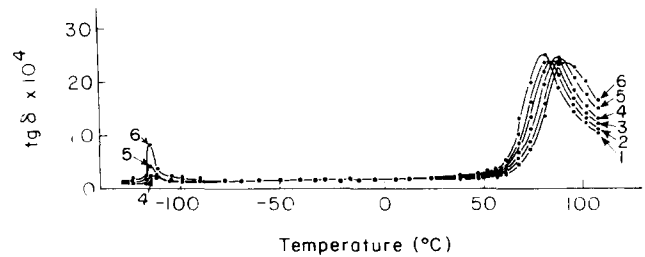


Figure 2 Dielectric isofrequency spectra of polyallylbenzene at low temperatures  $N$ : (1): 200 Hz; (2): 500 Hz; (3): 1 KHz; (4): 2 KHz; (5): 5 KHz; (6): 10 KHz

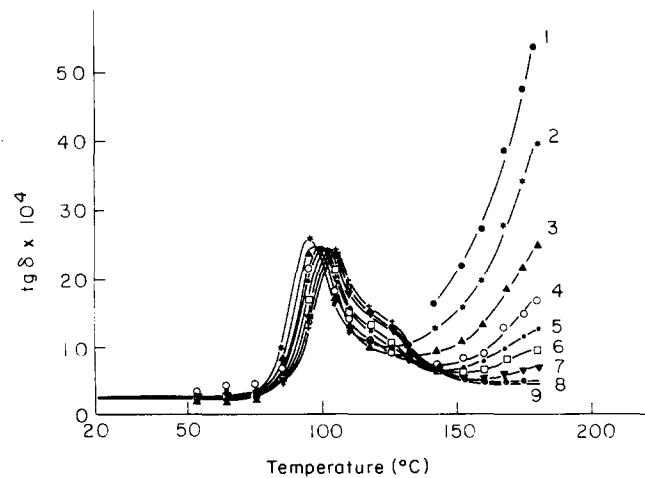


Figure 3 Dielectric isofrequency spectra of poly(allylbenzene) at high temperatures. (1), 30 Hz; (2), 70 Hz; (3), 200 Hz; (4), 500 Hz; (5), 1 kHz; (6), 2 kHz; (7), 5 kHz; (8), 7 kHz; (9), 10 kHz

chains due to the effect of a large substituent. Figure 3 shows the spectrum at high temperature of a film stored for one year after moulding. The peak of  $\beta$  relaxation has the same amplitude but is shifted by  $15^\circ\text{C}$  towards higher temperatures due to ageing. A broad shoulder in the  $120$ – $130^\circ\text{C}$  range suggests the existence of a double glass transition.

Above  $150^\circ\text{C}$ , the  $\text{tg } \delta$  curves rise sharply. The results of this type of experiment do not allow us to say if this is due to the liquid–liquid transition or due to the beginning of the  $\alpha$  relaxation associated with the motion of the crystalline phase at temperatures about the melting point.

### T.s.c. spectra

Figure 4 shows t.s.c. spectra of poly(allylbenzene)  $A_p$ . Those for poly(allylbenzene) film  $A_r$  are shown in Figures 5 and 6. We note, first, a relaxation around  $T = -120^\circ\text{C}$  designated  $\gamma$  and already observed in dielectric measurements, then a  $\beta$  relaxation around  $60^\circ\text{C}$  and finally a relaxation at higher temperature  $120$ – $130^\circ\text{C}$ .

### Thermal sampling

The experiments were carried out from the liquid nitrogen temperature up to the melting of the product both for  $A_p$  and  $A_r$ , to observe the influence of the melting of the polymer on its dielectric behaviour.

Figures 7 and 8 show as an example the elementary spectra for the glass transition region and for  $T_{11}$  of  $A_p$ . Each elementary spectrum is well described by a single

relaxation time ' $\tau$ '. The dependence of  $\tau$  on temperature can be described according to the behaviour of the material which can be explained through activated or unactivated processes.

The observed relaxations obey an Arrhenius equation for an activated process:

$$\tau(T) = \tau_0 \exp\left\{\frac{u}{kT}\right\} \quad (1)$$

where  $\tau_0$  is the pre-exponential factor and  $u$  the activation energy.

In the case of an unactivated process, the Vogel equation was proposed:

$$\tau(T) = \tau'_0 \exp\left\{\frac{1}{\alpha T - T_\infty}\right\} \quad (2)$$

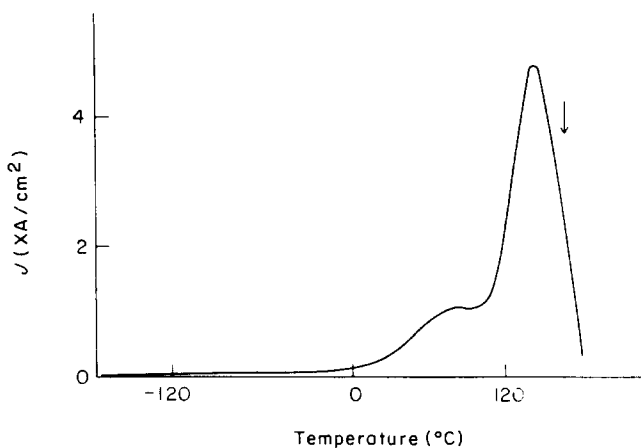


Figure 4 T.s.c. spectrum of poly(allylbenzene) powder:  $X = 10^{-11}$ ; the polarization temperature is indicated by arrow on the Figure

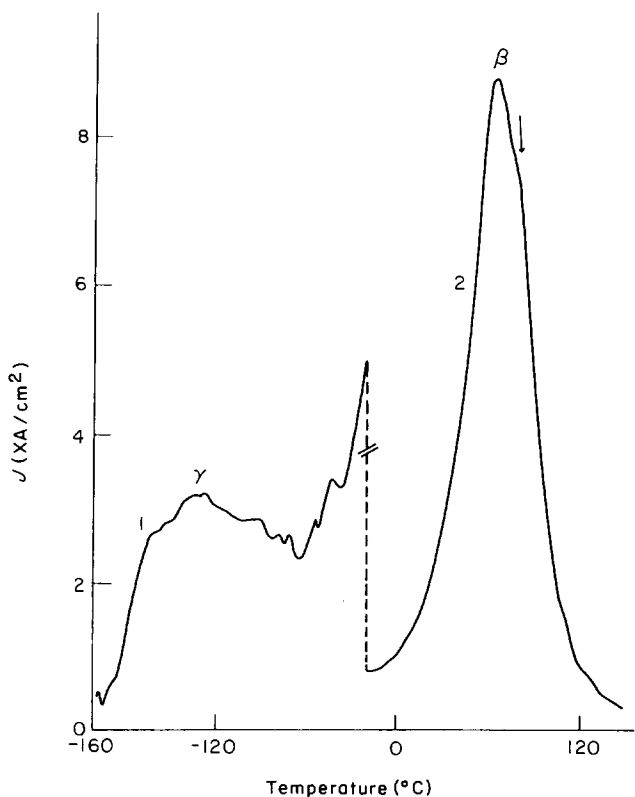


Figure 5 T.s.c. complex spectra of poly(allylbenzene) film. (1),  $X = 3 \times 10^{-13}$ ; (2),  $X = 3 \times 10^{-12}$ ; the polarization temperatures are indicated by small arrows on the figure

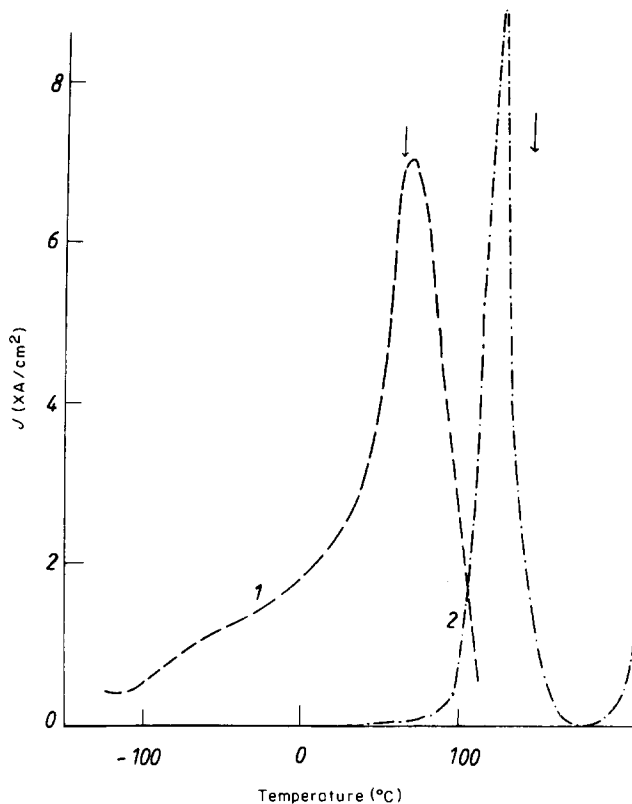


Figure 6 T.s.c. complex spectra of poly(allylbenzene) film. (1),  $X = 3 \times 10^{-12}$ ; (2),  $X = 3 \times 10^{-10}$ ; the polarization temperatures are indicated by small arrows on the figure

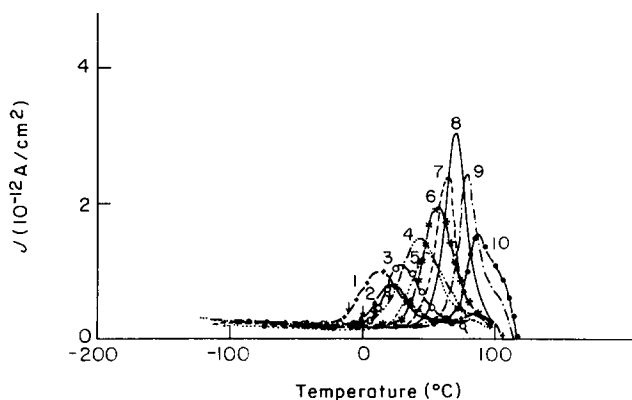
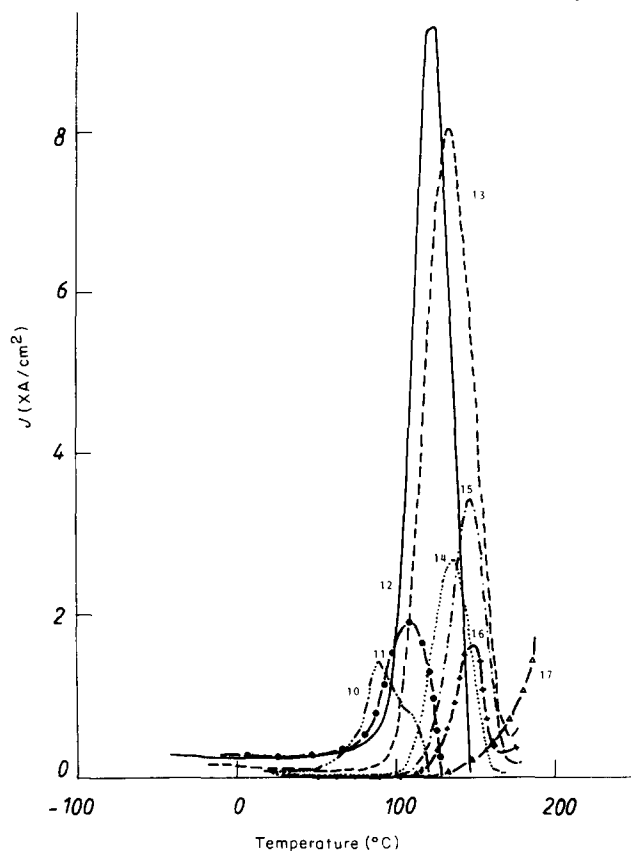


Figure 7 Thermal sampling spectra for  $A_p$ : glass transition region

where  $\tau'_0$  is the pre-exponential factor,  $\alpha$  the thermal expansion coefficient of the free volume and  $T_\infty$  the critical temperature; (2) linearizes the semi-logarithmic variation of  $P(T)/J(T)$  versus  $1/(T - T_\infty)$ . The discontinuity of the free volume is represented by  $T_\infty$ .

The plots  $\log \tau = f(1/T)$  for each elementary peak are reported in Figure 9. We consider first, the linear variations which are described by the Arrhenius equation (1). The associated values of  $\tau_0$  and  $u$  are reported in Table 1 for these elementary processes.

The temperature dependences of relaxation times for  $\beta$



**Figure 8** Thermal sampling spectra for  $A_p$ : liquid-liquid transition region; (10) (11) (12):  $X = 10^{-12}$ ; (13):  $X = 3 \times 10^{-12}$ ; (14) (15) (16) (17):  $X = 3 \times 10^{-11}$

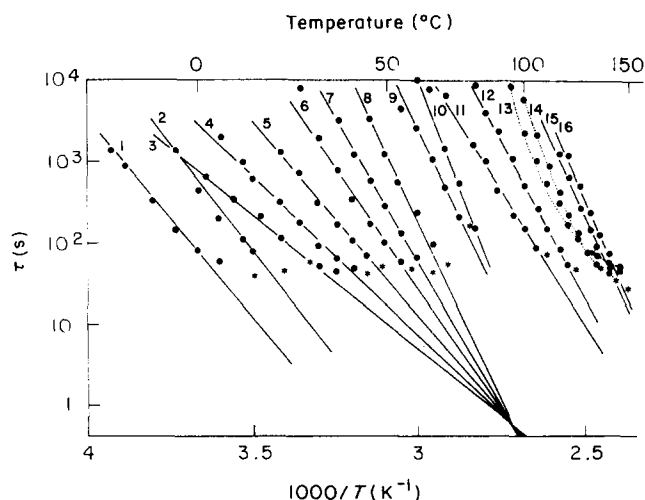


**Figure 9** Relaxation times as a function of reciprocal temperature from thermal sampling for  $A_p$

relaxation region (peaks 3–8, *Figure 9*) follow the compensation law described in equation (3).

$$\tau_i = \tau_c \exp\left\{\frac{\Delta H_i}{k}\right\} (T^{-1} - T_c^{-1}) \quad (3)$$

with  $T_c = 86^\circ\text{C}$  and  $\tau_c = 0.46$  s.

Such behaviour was previously observed in semi-crystalline polymers and attributed to the low temperature component of the glass transition  $T_{g(1)}$ . An empirical relationship was found between  $T_c$  and  $T_g^8$ .

$$T_g \sim T_c - 27^\circ\text{C} \quad (4)$$

**Table 1** T.s.c. data: parameters calculated from the thermal sampling (*Figures 7 and 8*) of  $A_p$ .  $T_p$  temperature of polarization;  $T_m$  temperature of the peak maximum

Attribution	Peak no.	$T_p$ (°C)	$T_m$ (°C)	Arrhenius process		Vogel process		
				$U$ (eV)	$\tau_0$ (s)	$\tau'_0$ (s)	$\alpha$ (°C <sup>-1</sup> )	$T_\infty$ (°C)
	1	-10	13					
	2	0	20	0.88	$1.98 \times 10^{-14}$			
$T_{g(l)}$	3	10	28	0.73	$3.15 \times 10^{-11}$			
	4	20	44	0.79	$7.1 \times 10^{-12}$			
	5	30	49	0.98	$1.94 \times 10^{-11}$			
	6	40	57	1.1	$2.2 \times 10^{-16}$			
	7	50	64	1.34	$3.3 \times 10^{-19}$			
	8	60	70	1.76	$3.3 \times 10^{-25}$			
$T_{g(l)}$	9	70	79	1.65	$2.2 \times 10^{-22}$			
	10	80	87	2.12	$9.5 \times 10^{-29}$			
$T_{g(l)}$	11	90	108	1.32	$1.95 \times 10^{-15}$			
	12	100	122	1.56	$4.7 \times 10^{-15}$			
$T_{ll0}$	13	110	133			0.0275	$12.5 \times 10^{-4}$	30
						0.0197	$11.4 \times 10^{-4}$	25
						0.010	$11.6 \times 10^{-4}$	35
	14	120	136			0.0050	$10.3 \times 10^{-4}$	30
						0.054	$9.6 \times 10^{-4}$	25
						0.016	$8.3 \times 10^{-4}$	20
$T_s$	15	130	144	1.7	$6.2 \times 10^{-20}$			
	16	140	149	1.9	$9.4 \times 10^{-22}$			

It lets us predict for poly(allylbenzene) powder:  $T_g \sim 59^\circ\text{C}$ .

Higher temperature relaxations  $\beta'$  (lines 10–12) can be attributed to the high temperature component of the glass transition  $T_{g(u)}$ .

The peaks observed at the highest temperatures (lines 15–16) can be assigned to the  $\alpha$  relaxation of the crystalline regions.

For the relaxation process observed after polarization at 110 and 120°C Figure 9, lines 13, 14 shows that Arrhenius law is not fulfilled and values of  $\tau_0$  are mistaken. For both cases a critical temperature  $T_\infty$  exists (25 and 30°C respectively) that linearizes the dependence of  $\ln \tau$  versus  $1/T - T_\infty$  (Figure 10). It means the relaxation times are well described by the Vogel equation (equation (2)). The thermal expansion coefficient calculated from this equation  $\alpha = 10 \times 10^{-4} \text{ c}^{-1}$  is in good agreement with the dilatometric data in the same temperature range<sup>3</sup>.

In the case of film  $A_f$ , the  $\beta$  relaxation presents the same behaviour as for  $A_p$  and the relaxation times obey a compensation law. The values of the parameters differ significantly with  $T_c = 76^\circ\text{C}$  and  $\tau_c = 3 \text{ s}$ . Equation (4) lets us predict a glass transition temperature  $T_g \sim 49^\circ\text{C}$ , i.e.  $10^\circ\text{C}$  lower than that for the powder. These data reveal that the low temperature glass transition  $T_{g(l)}$  is sensitive to the

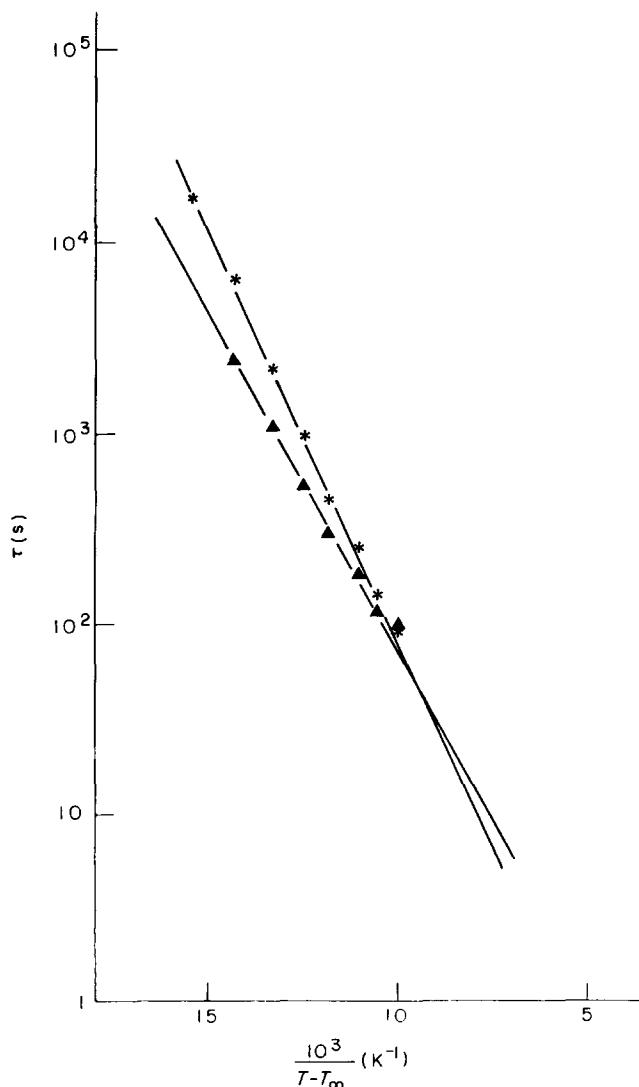


Figure 10 Semilogarithmic variation of the relaxation times versus  $10^3/(T - T_\infty)$  for the t.s.c. peak isolated at 133°C for peak (13) (▲) and for peak (14) (\*)

morphology<sup>9</sup> of the sample. In the range 110–120°C appears the relaxation  $\beta'$  associated with the high temperature component of the glass transition  $T_{g(u)}$ .

At high temperature, the relaxation processes obey a Vogel law. The linearizations are well fitted with the critical temperatures  $T_\infty = 25^\circ\text{C}$  and  $80^\circ\text{C}$ .

Thus the temperature range relaxations obey the Arrhenius or Vogel laws. In the latter case, the interpretation of the phenomena is complex because they can be related at the possibility of chain element motion<sup>10</sup> but they can also be related to the release of charge carriers or trapping which can occur with the increased mobility of the chains at high temperatures<sup>11,12</sup>.

Our polymeric system is a dielectric system and there is practically no possibility of the intrinsic generation of carriers. So the charge carriers must be injected from electrodes and trapped in the samples. They can be released during the heating of the specimen during the study and give the t.s.d. peak<sup>13</sup>. These possibilities are considered but taking into account the preparation of the sample and the measurements conditions, we have assigned the non-activated relaxations in the range 130–145°C to the chain motions at  $T_{li}$ : liquid–liquid transitions observed in the t.s.c. study.

The electrical results were analysed in terms of relaxation associated with molecular motions and the temperatures at which they occurred are reported in Table 2. The shift towards low temperatures of the relaxations of the film in relation to those of the powder indicates a different thermodynamic state of the product and conforms the previous results on thermal and physical effects<sup>3</sup>.  $\beta$  and  $\beta'$  relaxations are observed in the two cases but ' $\alpha$ ' appears only for  $A_p$ . The relaxations, which obey the Vogel law correspond to liquid–liquid transitions of the morphological domain defines with the two components of the  $T_g$ .

## DISCUSSION

The different results of structural characterization<sup>2</sup>, thermal<sup>3</sup> and dielectrical properties of poly(allylbenzene) give us the opportunity to propose a morphological model of this polymer in order to establish the origin of the observed transitions and to correlate structure and properties.

Poly(allylbenzene) does not present a superstructural organization (neither spherulitic or rod-like type in optical polarized microscopy or in small angle light scattering) or an orientation of chains under stretching. The crystallization of the polymer takes place from chains in stretched conformations according to the bulkiness of the phenyl groups. These groups have a certain mobility due to the methylene unit  $\text{CH}_2$  which determines very different properties for polyallylbenzene and polystyrene<sup>14</sup>. The probability of coupling of this phenyl ring is corroborated by a certain tacticity of the chain and the difficulty dissolving the polymer above  $T = 100^\circ\text{C}$  using aromatic or polar solvents<sup>2</sup>.

Table 2 Transition temperatures in polyallylbenzene

Poly(allylbenzene)	$T_{g(l)}$ (°C)	$T_{g(u)}$ (°C)	$T_{H(l)}$ (°C)	$T_{H(u)}$ (°C)	$T_\alpha$ (°C)
Powder	64	122	136	–	149
Film	59	118	133	144.5	–

### Morphological model

According to the previous remarks, we can say that polyallylbenzene is a semi-crystalline material with some islands of short range order corresponding to crystallites in a disorganized environment of chains (Figure 11). The possibility of  $\phi$ - $\phi$  coupling creates some weak networks called 'tangles' between chains of free amorphous zones or chains anchored to crystallites, i.e. in tied amorphous zones<sup>9</sup>.

So the chains have numerous possibilities of intra- or interchain couplings and can form 'microcrystallites'.

### Structure-transition relationship

The presence of a double glass transition is well explained by considering the existence of the two types of amorphous zones cited above.

(a)  $T_{g(l)}$  or low temperature glass transition associated with  $\beta$  relaxation would be connected with the micro-Brownian movements of the chains in the free amorphous zone and are not so easy in the raw synthesized polymer  $A_p$  or aged film as in fresh film  $A_f$ . The same remark was formulated during the d.t.a. or d.s.c.<sup>3</sup> measurements. It means that the mobility of the chains depends on the size, the number and the distance which separates the crystallites determined by the thermal history of the samples.

(b)  $T_{g(u)}$  or high temperature glass transition associated with  $\beta'$  relaxation would be connected with the 'tied amorphous zone'. Undergoing stronger constraints due to anchored points from the crystalline zone, the chains move at higher temperature. The second component of  $T_g$  corresponds also to the shoulder of the  $\beta$  relaxation peak in Figure 3 and certainly its temperature determines the different conductivity behaviour of the material.  $T_{g(u)}$  was also detected in inverse gas chromatography.

The movements of the chains of the two amorphous

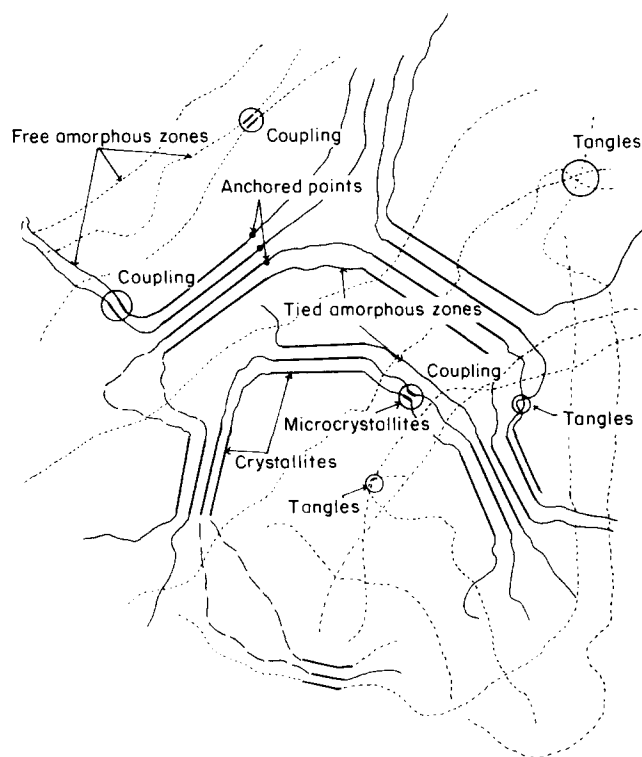


Figure 11 Morphological model of poly(allylbenzene)

zones are liberated above 120°C. In fact their stiffness is decreased through the modifications of a certain number of phenyl-phenyl interactions. This is seen from the infra-red analysis at high temperature, for which the spectra show absorption modifications corresponding to characteristic vibrations of aromatic groups towards 110°C. This temperature agrees too, with the solubilization temperature of the polymer in aromatic and polar solvents<sup>2</sup>. The latter have a greater possibility of approaching the chains and can help to break the interchain bondings by coupling themselves with phenyl groups of the polymer.

(c)  $T_{ll(l)}$  the low temperature component of this liquid-liquid transition would correspond to the fluidization of the chains of the free amorphous zone, owing to new decrease of the interchain interactions of this phase. The observed gap of temperature of  $T_{ll(l)}$  between the powder and the film corresponds to that observed for  $T_{g(l)}$ .

(d)  $T_{ll(u)}$  or high temperature liquid-liquid transition would be the result of a decrease of all the interactions, present in the tied amorphous zone, as in the inter-crystalline zone. It does not appear in  $A_p$  because it might occur at a higher temperature depending upon the morphology<sup>15</sup>.

In fact the material sufficiently liquid near 150°C can organize again, because of a marked decrease of the constraints due to coupling tangles or anchored points, which leads to the volume shrinkage noted in dilatometric study<sup>16</sup> or explains the flat curve of the plots in t.m.a. On another hand, the thermal spectra of d.t.a. and d.s.c. reveal a beginning of 'fusion' at about this temperature.

(e) Another transition,  $T_x$ , associated with relaxation  $\alpha$  and attributed to the melting of the microcrystallites formed in the tied amorphous zone is observed for  $A_p$  at high temperatures.

The film does not show the same behaviour. It was moulded at 204°C and cooled very slowly. So, the crystallites, which have grown, are much bigger and less numerous than those of the powder. The tied amorphous zone takes certainly a place not so large and has not the possibility of organizing itself to relax at  $T_x$ .

### CONCLUSION

It is well-known that the determinations of glass and liquid-liquid transition temperatures of a polymer are influenced by the types of techniques used<sup>17</sup>. So it is important to note that the set of data presented here is consistent. The high resolving power of the t.s.c. technique allows us to show that the glass and liquid-liquid transitions of poly(allylbenzene) have two components that were related to morphological entities of the polymer and the evolution of the crystalline domains.

We hope that this work on poly(allylbenzene) will contribute to the understanding of the physical behaviour of new or modified<sup>18</sup> materials.

### REFERENCES

- 1 Boiteux, G., Seytre, G., Berticat, P., Merle, G. and Dubois, J. C. *Makromol. Chem.* 1979, **180**, 761
- 2 Boiteux-Steffan, G. and Pham, Q. T. *Makromol. Chem.* 1984, **185**, 877
- 3 Boiteux-Steffan, G., Letoffé, J. M., Sage, D. and Soulier, J. P. *Polymer* 1985, **26**, 1443

*Multiple transitions in poly(allylbenzene). 2: G. Boiteux-Steffan et al.*

- 4 Boiteux-Steffan, G. *PhD Thesis*, University of Lyon (1981)
- 5 Lacabanne, C., Chatain, D., Guillet, J., Seytre, G. and May, J. F. *J. Polym. Sci. Phys. Edn.* 1975, **13**, 445
- 6 Karasz, F. E. 'Dielectric Properties of Polymers', Plenum Press, New York, London (1972)
- 7 Nozaki, M. and Shimada, K. *J. Appl. Phys.* 1970, **9**, 843
- 8 Monpagens, J. P. *PhD Thesis*, University of Toulouse (1977)
- 9 Boyer, R. F. in 'Transitions and relaxations in amorphous and semicrystalline organic polymers and copolymers, Encyclopedia of Polymer Science and Technology, Suppl.', Vol. II, pp. 745-839, John Wiley (1977)
- 10 Vanderschuren, J., Janssens, A., Ladang, M. and Niezette, J. *Polymer* 1982, **23**, 395
- 11 Van Turnhout, J. in 'Thermally Stimulated Discharge of Polymer Electrets', Elsevier, Amsterdam, 1975
- 12 Marchal, E. *C.R. Acad. Sci. Paris* 1983, **297**, 2, 713
- 13 Kryszewski, M., Ulanski, J., Jeszka, J. K. and Zielinski, M. *Polym. Bull.* 1977, **8**, 187
- 14 Seefried, C. G., Koleske, J. R. and Koleske, J. V. *J. Polym. Sci.* 1976, **14**, 663
- 15 Goyaud, P. *PhD Thesis*, University of Toulouse (1979)
- 16 Gillham, J. K. and Boyer, R. F. *J. Macrom. Sci. Phys.* 1977, **B13**, 497
- 17 Boyer, R. F. *Polym. Eng. Sci.* 1979, **19**, 732
- 18 Boiteux-Steffan, G., Berticat, P., Lucas, J. M. and Seytre, G. *Europ. Polym. J.* 1983, **19**, 171